nature microbiology

ARTICLES

https://doi.org/10.1038/s41564-018-0248-x

Peptidoglycan editing by a specific LD-transpeptidase controls the muramidase-dependent secretion of typhoid toxin

Tobias Geiger[1], Manuel Pazos[2], Maria Lara-Tejero[1], Waldemar Vollmer[2] and Jorge E. Galán[1]*

Protein secretion mechanisms are essential for the virulence of most bacterial pathogens. Typhoid toxin is an essential virulence factor for Salmonella Typhi, the cause of typhoid fever in humans. This toxin is unique in that it is only produced within mammalian cells, and it must be trafficked to the extracellular space before intoxicating target cells. An essential and poorly understood aspect of this transport pathway is the secretion of typhoid toxin from the bacterium into the S. Typhi-containing vacuole. We show here that typhoid toxin secretion requires its translocation to the trans side of the peptidoglycan layer at the bacterial poles for subsequent release through the outer membrane. This translocation process depends on a specialized muramidase, the activity of which requires the localized editing of peptidoglycan by a specific ld-transpeptidase. These studies describe a protein export mechanism that is probably conserved in other bacterial species.

Bacterial pathogens have evolved sophisticated protein secretion systems that can direct proteins to the extracellular environment or even directly into eukaryotic cells[1–4]. Protein transport across the bacterial envelope is particularly challenging in Gram-negative bacteria, as proteins must move through at least three barriers: the inner membrane, the peptidoglycan (PG) layer and the outer membrane. The Gram-negative bacterial pathogen *Salmonella enterica* serovar Typhi (*S.* Typhi) is the cause of typhoid fever, a systemic disease of humans that remains a global health concern[5–9]. Typhoid toxin is an essential virulence factor of this pathogen and it is believed to be largely responsible for the acute, life-threatening symptoms of typhoid fever[10–12]. This toxin, which is encoded within a discrete genomic islet (Supplementary Fig. 1), has a unique A_2B_5 architecture with two covalently linked enzymatic 'A' subunits, PltA and CdtB, associated to a homopentameric 'B' subunit made up of PltB (ref. [11]). A unique feature of typhoid toxin is that it is exclusively expressed by intracellularly localized bacteria[10,13,14]. This unique pattern of gene expression is the result of a silencing and counter-silencing transcriptional regulatory mechanism through the opposing actions of the PhoP/PhoQ two-component regulatory system and the histone-like protein H-NS[14]. Once synthesized and exported to the periplasmic space by the *sec*-dependent pathway, the toxin is assembled into a 115 kDa multimeric complex, which is secreted into the lumen of the *S.* Typhi-containing vacuole. The toxin is then packaged into vesicle carrier intermediates, which transport it to the extracellular space from where it can reach its targets[10,15]. The mechanism by which the toxin is secreted from the bacteria into the lumen of its enclosing phagocytic vacuole is not understood, although it is known to require *ttsA*, which is located within the same locus as the typhoid toxin genes (Supplementary Fig. 1), and encodes a homologue of bacteriophage *N*-acetyl-β-D-muramidases[16]. Here we show that TtsA mediates the translocation of typhoid toxin from the *cis* to the *trans* side of the PG layer, positioning the toxin within a compartment from where it can be rapidly released by membrane active compounds encountered by *S.* Typhi during infection. We found that TtsA activity requires the editing of the PG at the bacterial poles by a specific LD-transpeptidase, which is essential for toxin secretion. This study describes a protein export mechanism, which has evolved to ensure the release of a toxin in the appropriate environment.

Results

TtsA-dependent translocation and agonist-mediated release of typhoid toxin after *S.* Typhi growth in vitro. Because typhoid toxin is exclusively produced within infected cells, visualization of vesicle carrier intermediates has been the only surrogate assay available to study typhoid toxin secretion (Supplementary Fig. 2)[16], and this assay is poorly suited for mechanistic studies. We have recently unravelled the regulatory network that controls the exclusive intracellular expression of typhoid toxin[14], allowing us to identify in vitro culture conditions that closely mimic those encountered by bacteria within mammalian cells[17] and that are therefore permissive for typhoid toxin and TtsA expression at levels equivalent to those in infected cells (Fig. 1a and Supplementary Fig. 2)[14,16,18]. Using these growth conditions (henceforth referred to as 'typhoid toxin inducing media' or TTIM), we examined the TtsA-dependent secretion of typhoid toxin into culture supernatants monitored through the detection of its CdtB subunit. Surprisingly, we did not detect typhoid toxin in culture supernatants or on the surface of bacteria grown under these conditions, although we readily detected it in whole bacterial lysates (Fig. 1b,c). However, we found that the addition of a very low amount of detergent to bacterial cells, which did not affect viability (Supplementary Fig. 3), resulted in the detection of typhoid toxin both in the supernatants (Fig. 1b) and on the bacterial cells (Fig. 1c). The detection of the toxin in these locations was strictly dependent on TtsA function, because it was not detected on *S.* Typhi Δ*ttsA* bacterial cells (Fig. 1d,e and Supplementary Data Set 1) or supernatants (Fig. 1b) after its growth in TTIM, even though the toxin levels of expression in the Δ*ttsA* mutant and wild-type strains were indistinguishable (Fig. 1f). Intracellular bacteria, particularly those that, like *S.* Typhi, inhabit lysosome-related organelles[18], are exposed to a myriad of membrane-disrupting compounds such as antimicrobial

[1]Department of Microbial Pathogenesis, Yale University School of Medicine, New Haven, CT, USA. [2]The Centre for Bacterial Cell Biology, Institute for Cell and Molecular Biosciences, Newcastle University, Newcastle upon Tyne, UK. *e-mail: jorge.galan@yale.edu

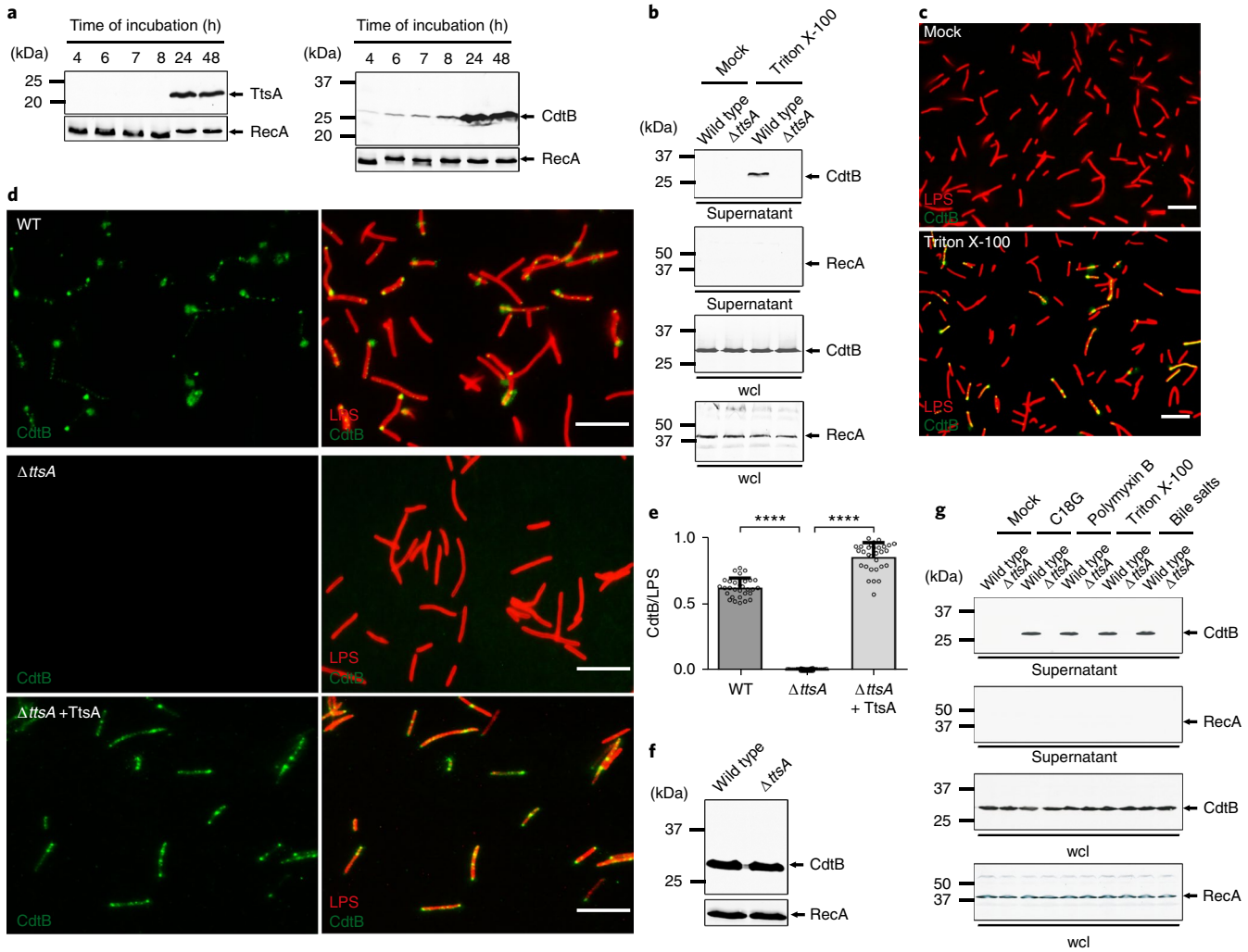

Fig. 1 | TtsA-dependent translocation and agonist-mediated release of typhoid toxin in vitro. a, Expression of TtsA and typhoid toxin in TTIM. *S.* Typhi carrying chromosomally encoded FLAG-tagged CdtB (as a surrogate for typhoid toxin) or TtsA were grown in TTIM and the expression of TtsA and CdtB in equal numbers of bacterial cells was monitored over time by western blot analysis. The amount of RecA (loading control) was analysed on a separate western blot. **b**–**e**, Outer membrane disruption results in the TtsA-dependent detection of typhoid toxin in culture supernatants and on bacterial cells. Wild-type and Δ*ttsA S.* Typhi (CdtB-FLAG) were grown in TTIM for 24 h, pelleted, and washed twice with PBS, then treated with Triton X-100 (0.1%). Bacterial whole-cell lysates (wcl) and filtered culture supernatants were then analysed by western blotting for the presence of CdtB and RecA (as a cell lysis and loading control) (**b**). Alternatively, wild-type *S.* Typhi was grown for 24 h in TTIM, fixed, treated with Triton X-100 (0.1%) or PBS (mock), and then stained with mouse anti-FLAG (to stain CdtB) (green) and rabbit anti *S.* Typhi lipopolysaccharides (LPS) (to visualize bacterial cells) (red) (**c**). The indicated strains in **d** and **e** (grown in the same manner) were fixed, treated with Triton X-100 (0.1%) and stained as indicated under (**c**). The average ratios of typhoid-toxin-positive cells (green) versus total cells (LPS, red) ± s.d. are shown (****$P < 0.0001$, two-sided Student's *t*-test) (Supplementary Data Set 1) (**e**). The levels of CdtB in the strains used in **c** were determined by western blot analysis using RecA as a loading control analysed on a separate western blot (**f**). **g**, Antimicrobial peptides trigger the release of typhoid toxin to the culture supernatants. Wild-type and Δ*ttsA S.* Typhi strains (CdtB-FLAG) CdtB were grown for 24 h in TTIM, pelleted, and washed twice with PBS, then treated with sub-inhibitory concentrations of antimicrobial peptide C18G (2.5 μg ml^{-1}), polymyxin B (0.1 μg ml^{-1}), Triton X-100 (0.1%) or bile salts (0.05%). Filtered supernatants and whole-cell lysates were analysed by western blotting for the presence of CdtB and RecA (as a cell lysis and loading control). All data in **a**–**g** were derived from at least three independent experiments. Scale bars (**c**,**d**), 5 μm.

peptides, or membrane active proteins such as those of the saposin or perforin families[19–21]. *S.* Typhi, in particular, is known to colonize the gallbladder and to form biofilms in gallbladder stones[22,23], which would readily expose it to bile salts. We hypothesized that, similarly to Triton X-100, these compounds could act as stimulators of toxin release. In fact, we have previously shown that sub-inhibitory concentrations of antimicrobial peptides can stimulate typhoid toxin expression[14]. We therefore tested whether the addition of antimicrobial peptides or bile salts could trigger typhoid toxin release to cell-free supernatants after *S.* Typhi growth in TTIM. Western blot analysis indicated that the addition of antimicrobial peptides C18G, polymyxin B or bile salts at concentrations that did not inhibit *S.* Typhi growth (Supplementary Fig. 3) stimulated the rapid release of up to ~20% of the total typhoid toxin pool in wild-type *S.* Typhi but not in its isogenic Δ*ttsA* mutant grown under the same conditions (Fig. 1g). We also utilized liquid chromatography–tandem mass spectrometry (LC–MS/MS) to examine the cell-free supernatants of wild-type and Δ*ttsA S.* Typhi grown in TTIM after stimulation with the same agonists. We found that the addition of antimicrobial peptides C18G, polymyxin B or bile salts resulted in the selective

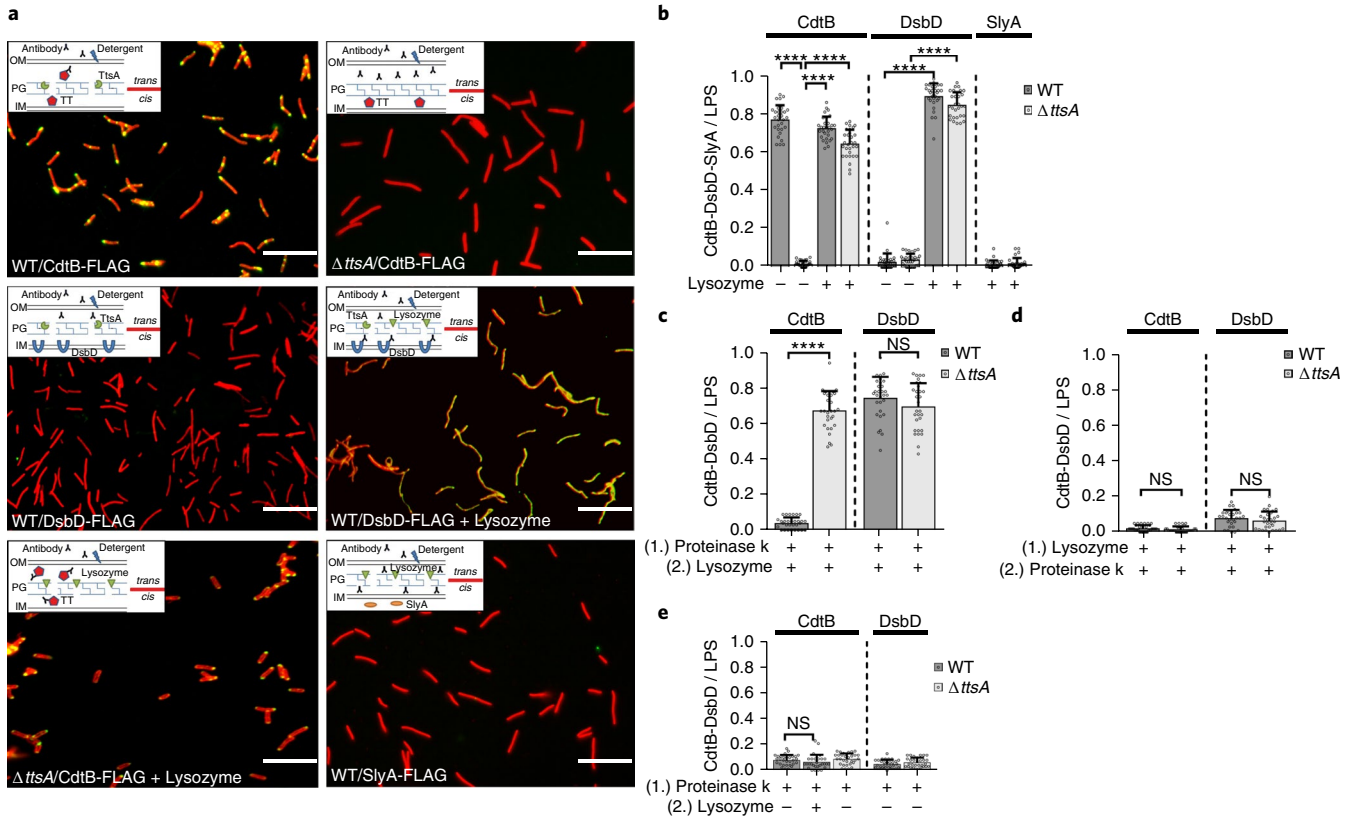

Fig. 2 | TtsA mediates the transport of typhoid toxin to the *trans* side of the PG layer. a–e, Wild-type and Δ*ttsA S.* Typhi carrying chromosomally encoded FLAG-tagged CdtB (as a surrogate for typhoid toxin), DsbD or SlyA (as indicated) were grown in TTIM for 24 h, fixed, mock-treated or treated with lysozyme for 20 min (to permeabilize the PG layer), and stained as in Fig. 1c. To probe the TtsA-dependent translocation of typhoid toxin from the *cis* to the *trans* side of the PG layer, bacteria (wild-type and Δ*ttsA* mutant) were first treated with proteinase K for 30 min, followed by lysozyme or mock treatment for 20 min (**c**,**e**), or first treated with lysozyme for 20 min, followed by proteinase K treatment for 30 min (**d**). In all cases, the number of bacterial cells positive for CdtB, DsbD or SlyA signals (green) was quantified relative to the total number of bacteria analysed (LPS, red signal). Average ratios of green positive cells to red total cells ± s.d. from three independent experiments are shown. In all cases, a total of 30 images were collected from which 100 randomly selected bacteria (total number) per image were analysed, resulting in 3,000 bacterial cells analysed per bacterial strain or condition (****$P < 0.0001$; **c**, not significant (NS) $P = 0.131$, **d**, NS $P = 0.2078$, $P = 0.28$, **e**, NS $P = 0.2646$, two-sided Student's *t*-test) (Supplementary Data Set 2) (**b**–**e**). Scale bars (**a**), 5 μm. OM, outer membrane; IM, inner membrane.

release of typhoid toxin into the cell-free supernatants of wild-type bacteria, as no other resident periplasmic proteins were detected by our analysis (Supplementary Data Set 6). Consistent with western blot analysis, typhoid toxin was not detected by LC–MS/MS in cell-free supernatants of the *S.* Typhi Δ*ttsA* mutant strain under any condition. These results indicate that the TtsA-mediated translocation of typhoid toxin through the PG layer must position the toxin at a subcellular site from where it can be subsequently released on receipt of the appropriate stimuli.

TtsA mediates the transport of typhoid toxin to the *trans* side of the PG layer. To characterize the subcellular compartment from which typhoid toxin is released to the extracellular space, we investigated its subcellular location in bacterial cells grown in vitro using immunofluorescence microscopy and different membrane permeabilization protocols. We found that, in contrast to wild-type, typhoid toxin could not be detected on the *S.* Typhi Δ*ttsA* mutant cells even after treatment with a higher concentration of Triton X-100 (1%) than that required for its release from wild-type bacteria (0.1%) (Fig. 2a,b). Under these conditions, the inner-membrane-anchored periplasmic protein DsbD epitope tagged at its periplasmic C terminus[24] could not be detected by antibody staining in wild-type *S.* Typhi (Fig. 2a,b). This observation indicates that in the absence of TtsA, typhoid toxin, like DsbD, is located on the *cis* side of the PG layer, inaccessible to antibody molecules. Consistent with this hypothesis, disruption of the PG layer by lysozyme treatment resulted in the detection on the bacterial cell of both typhoid toxin and DsbD, in the presence or absence of TtsA (Fig. 2a,b and Supplementary Data Set 2). These experimental conditions did not result in the detection of a cytoplasmic control protein (Fig. 2a,b and Supplementary Fig. 4), indicating that although the treatment disrupted the outer membrane and PG layer, it did not allow access of the antibody to the bacterial cytoplasm, a measure of an intact inner membrane. These results indicate that TtsA allows the translocation of typhoid toxin to the *trans* side of the PG layer, a location where it becomes accessible to antibody molecules after a minor disruption of the outer membrane. In the absence of TtsA, typhoid toxin remains in the *cis* side of the PG layer, where it is inaccessible to antibody molecules even after disruption of the outer membrane. To further probe this hypothesis, we carried out proteinase K susceptibility studies after different permeabilization protocols. We found that although proteinase K treatment of wild-type *S.* Typhi cells readily eliminated the detection of typhoid toxin, it did not affect the detection of the control protein DsbD, or typhoid toxin, in a Δ*ttsA* mutant *S.* Typhi (Fig. 2c and Supplementary Data Set 2). However, disruption of the PG layer by lysozyme pretreatment completely abolished the detection of DsbD and typhoid toxin in both wild-type or Δ*ttsA S.* Typhi after

addition of proteinase K (Fig. 2d and Supplementary Data Set 2). Taken together, these results demonstrate that (1) typhoid toxin resides in a compartment different from the compartment harbouring the canonical periplasmic protein DsbD; (2) these compartments are separated by the PG layer; (3) typhoid toxin resides in the *trans* side of the PG layer. Notably, in wild-type bacteria, proteinase K treatment without addition of lysozyme resulted in the removal of the entire population of typhoid toxin (Fig. 2e and Supplementary Data Set 2), indicating that the bulk of typhoid toxin molecules are located on the *trans* side of the PG layer, thus arguing that the TtsA-dependent toxin translocation process must be highly efficient.

Typhoid toxin and TtsA localize to the bacterial poles. During execution of these experiments, we noticed that typhoid toxin was preferentially detected at the bacterial poles. We therefore quantified the distribution of the typhoid toxin components CdtB and PltB using immunofluorescence microscopy and image analysis. We found a strong polar localization for both proteins (Fig. 3a, Supplementary Fig. 5 and Supplementary Data Set 3). Furthermore, the polar localization was also observed in intracellular bacteria after infection of cultured epithelial cells (Fig. 3b, Supplementary Fig. 5 and Supplementary Data Set 3). The localization of typhoid toxin at the bacterial poles was confirmed by live imaging of GFP-tagged CdtB (Supplementary Fig. 6) and by immunoelectron microscopy both in bacteria grown in TTIM, as well as in bacteria within cultured epithelial cells (Supplementary Fig. 7). We also examined the localization of TtsA both after growth in vitro and after bacterial infection in vivo. We found that, like typhoid toxin, TtsA is also localized at the bacterial poles (Fig. 3a,b and Supplementary Data Set 3). These results indicate that typhoid toxin is probably translocated at the bacterial poles and that the activity of TtsA may be selectively exerted at a discrete site of the bacterial envelope.

TtsA exerts its activity at the bacterial poles. The polar localization of TtsA suggested that its activity might be exerted at the bacterial poles, in which case TtsA-dependent PG remodelling should be detectable at these sites. To test this hypothesis we labelled the *S.* Typhi PG using an alkyne-modified D-alanine and an azide-containing fluorophore that can be linked by click chemistry[25]. The PG structure features linear glycan strands connected by short peptides, which contain D-alanine residues[26–28]. Consequently, metabolic incorporation of alkyne-modified D-alanine can be used to label remodelling PG[25,29,30]. We found that after a short (5 min) alkyne-D-alanine labelling pulse in exponentially growing *S.* Typhi, labelled PG could be readily visualized at the cell division septum (Supplementary Fig. 8). As expected, a long (60 min) labelling pulse led to PG labelling all around the entire body of the bacteria (Supplementary Fig. 8). These results confirmed that this approach can be used to detect PG remodelling in *S.* Typhi, and therefore we used it to label PG after growth to stationary phase in TTIM, conditions that lead to TtsA and typhoid toxin expression. We found that, in contrast to what we observed after logarithmic growth in LB broth, when *S.* Typhi was grown to stationary phase in TTIM for 24 h followed by an additional 4 h of growth in the presence of alkyne-D-alanine, PG labelling was preponderantly detected at the poles of the bacteria (Fig. 4a, Supplementary Fig. 9 and Supplementary Data Set 4). Importantly, in the *S.* Typhi Δ*ttsA* mutant we observed markedly reduced labelling, which was distributed throughout the body of the bacteria rather than concentrated at the poles (Fig. 4a, Supplementary Fig. 9 and Supplementary Data Set 4). These results indicate that when *S.* Typhi is grown under conditions that lead to typhoid toxin expression, TtsA exerts its activity on PG located at the bacterial poles, resulting in PG remodelling, probably as a result of the repair process that may follow its PG hydrolytic action.

To gain insight into the mechanisms that may restrict the activity of TtsA at the poles we examined the fate of TtsA and PG remodelling at the poles of bacteria that had been allowed to re-enter the cell cycle (conditions not permissive for TtsA activity), after growth to stationary phase (conditions permissive for TtsA expression and activity). We grew *S.* Typhi to stationary phase in TTIM and labelled the bacterial cultures with alkyne-D-alanine as described above. After 4 h of growth in the presence of alkyne-D-alanine, we split the cultures and added either casamino acids, which stimulate re-entry of the bacteria into the logarithmic phase of growth (Supplementary Fig. 10), or eluent (mock), and further grew the cultures for various times (always in the presence of alkyne-D-alanine). We found that, in the presence of casamino acids, the alkyne-D-alanine-dependent fluorescent signal at the poles was significantly diminished over time (Fig. 4b and Supplementary Data Set 4), even though under these conditions TtsA remained at the poles (Fig. 4d, Supplementary Fig. 11 and Supplementary Data Set 4). In contrast, in cultures without casamino acids, the fluorescent signal was readily detected at the poles (Fig. 4c). Taken together these results indicate that the presence of TtsA at the bacterial poles is not sufficient to induce polar PG remodelling and that a specific PG structure may be required for TtsA to exert its activity.

YcbB-dependent PG editing is required for typhoid toxin translocation across the bacterial envelope. The glycan strands that form the PG layer are connected by short 6- to 9-amino-acid peptides to maintain the rigidity of the cell wall[26–28]. The peptides contain L- and D-amino acids and in Gram-negative bacterial species like *S.* Typhi, the nascent peptide sequence is L-Ala–D-Glu–*m*-DAP (*meso*-diaminopimelic acid)–D-Ala–D-Ala. Some of the peptides are crosslinked by transpeptidase enzymes, including the so-called penicillin-binding proteins (PBPs), which produce the most commonly observed crosslinks between the carboxyl group of D-Ala at position 4 of one peptide to the ε-amino group of the *m*-DAP residue at position 3 of another (the so-called 4–3 or DD-crosslinks)[31]. Other minor crosslinks between two *m*-DAP residues of adjacent stem peptides (the so-called 3–3 or LD-crosslinks) are also observed, which in exponentially growing cells amount to only ~2% of all crosslinks, but in stationary phase or in intracellular bacteria can account for as much as ~20% of all crosslinks[31–33]. These crosslinks are catalysed by LD-transpeptidases, which are structurally and functionally unrelated to PBPs[34,35]. Unlike DD-transpeptidases, LD-transpeptidases are non-essential for growth. The activities of PG hydrolases are often dependent on specific modifications of the PG chain imparted by various enzymes including transpeptidases[36]. Our observation that the TtsA activity may depend on specific structural features of the PG subunits prompted us to investigate the potential contribution of LD-transpeptidases to typhoid toxin secretion. *S.* Typhi encodes four LD-transpeptidases: YbiS, ErfK, YcfS, which crosslink the PG to Braun's lipoprotein[34], and YcbB, which catalyses the formation of a direct link between two *m*-DAP residues[35]. A homologue of *ynhG*, which encodes another enzyme with this activity, is a pseudogene in *S.* Typhi. We found that introduction of deletion mutations in *ybiS, erfK, ycfS*, alone or in combination, had no effect on typhoid toxin secretion (Fig. 5a,b and Supplementary Data Set 5). However, introduction of a deletion in *ycbB* completely abolished typhoid toxin secretion, both in vitro (Fig. 5c and Supplementary Data Set 5) and after bacterial infection of cultured cells (Fig. 5d and Supplementary Data Set 5), although the introduction of any of the mutations did not affect typhoid toxin expression (Supplementary Fig. 12). The contribution of YcbB to typhoid toxin secretion was dependent on its catalytic activity because expression of the catalytic mutant $YcbB^{C528A}$ was unable to complement a Δ*ycbB S.* Typhi mutant strain (Fig. 5c,d and Supplementary Data Set 5). These results suggest that YcbB imparts localized PG modifications that are essential for TtsA activity. Consistent with this hypothesis, we found that the TtsA-dependent polar remodelling of the PG was strictly dependent

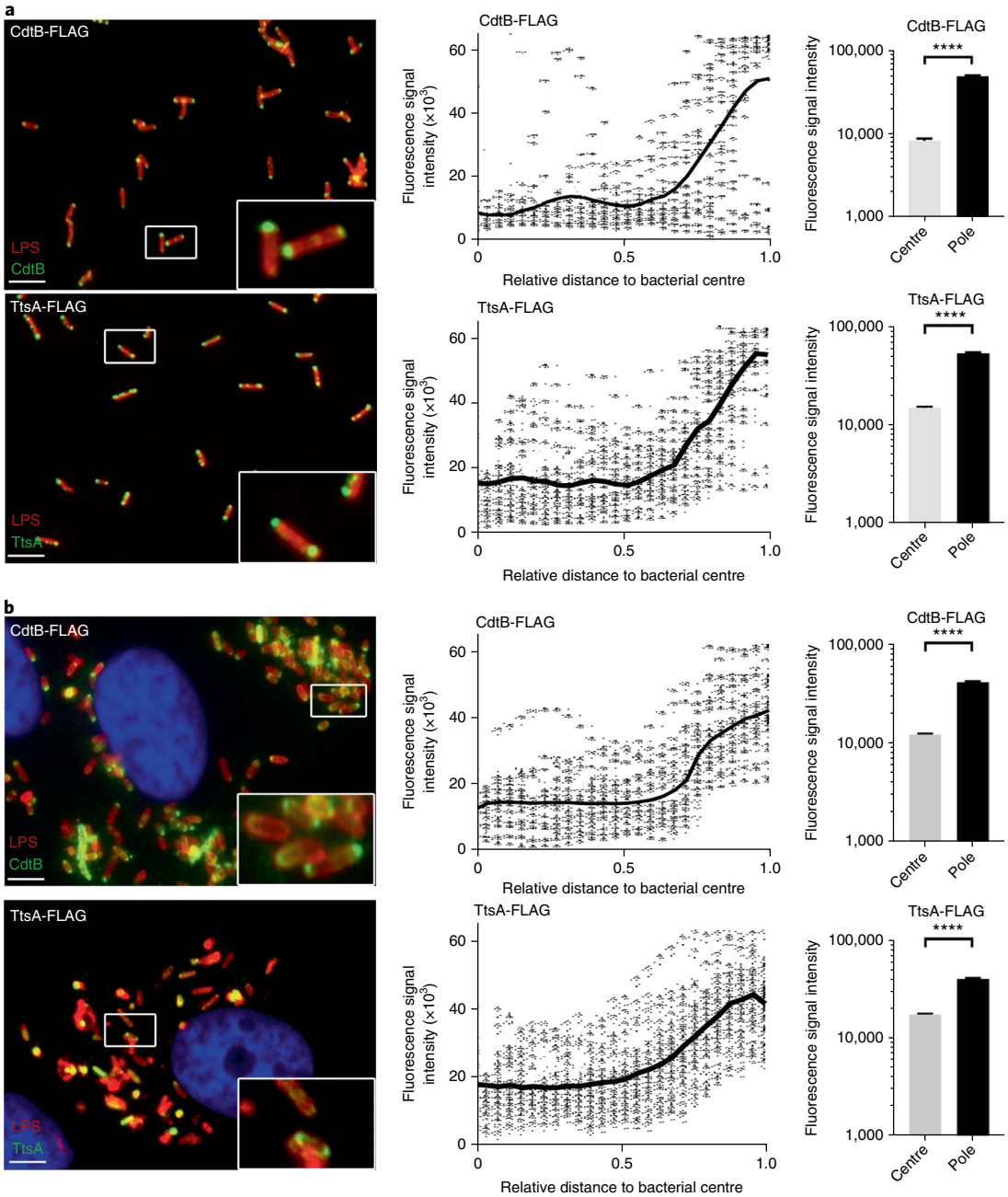

Fig. 3 | Typhoid toxin and TtsA localize to the bacterial poles. a,**b**, Typhoid toxin and TtsA localize to the bacterial poles after in vitro growth or cell infection. *S.* Typhi strains carrying chromosomally encoded FLAG-tagged CdtB (as a surrogate for typhoid toxin) or TtsA were grown for 24 h in TTIM, fixed, and stained with a mouse antibody directed to the FLAG-epitope (green) (to visualize CdtB or TtsA, as indicated) and a rabbit antibody directed to *S.* Typhi LPS (red) (**a**). Alternatively, the same *S.* Typhi strains were grown in LB (non-inducing medium), applied to cultured Henle-407 human epithelial cells, and 24 h post infection the infected cells were stained with an antibody directed to the FLAG-epitope (green) to visualize CdtB or TtsA (as indicated), a rabbit antibody directed to *S.* Typhi LPS (red), and DAPI for DNA detection (blue) (**b**). The scatter blot diagrams of each panel show fluorescence signal intensities for the corresponding FLAG-tagged protein distributed along the axes of individual bacterial cells. Twenty-six measuring points were defined from the centre (0) to each of the poles (1.0) of the bacterial cells, and the distribution of the fluorescence intensity along the axes of bacteria was analysed with the MicrobeJ plug-in of ImageJ (https://imagej.nih.gov/ij). The black line depicts the average of the intensities measured at each of the 26 measuring points. Data in each panel are from 1,800 individual measurements at each of the measuring points from 900 bacteria analysed in opposite directions from the centre. The bar graphs show the quantification of the signal intensities at the measuring point furthest from the centre (1.0), and at the centre of each bacterium (0) for each condition. Data presented as mean ± s.e m. from 1,800 measurements (****$P < 0.0001$, two-sided Student's *t*-test) (Supplementary Data Set 3). Scale bars (**a**,**b**), 5 µm.

on YcbB (Fig. 5e, Supplementary Fig. 13 and Supplementary Data Set 5), and that YcbB itself was enriched at the bacterial poles (Fig. 5f and Supplementary Data Set 5).

YcbB-edited PG is a substrate for TtsA activity. To further explore the mechanisms for TtsA specificity, we compared the PG structures of wild-type and Δ*ycbB S.* Typhi strains grown in TTIM,

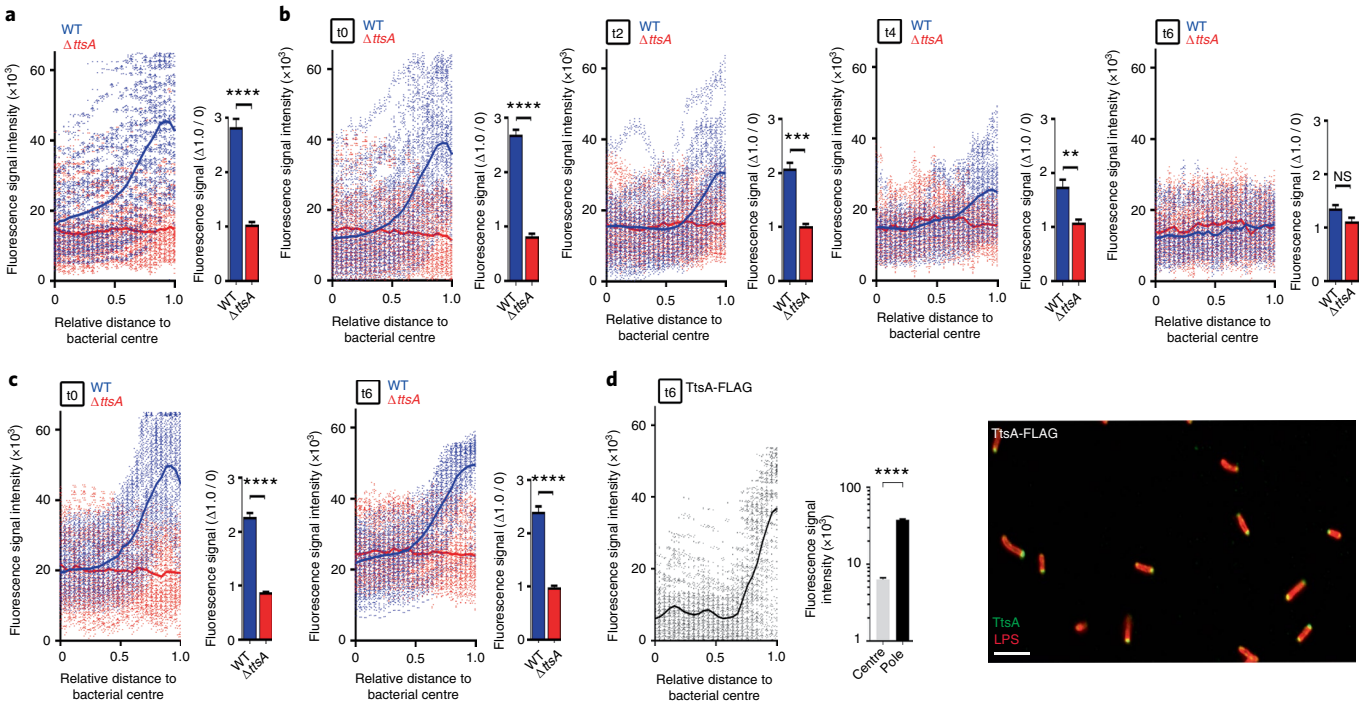

Fig. 4 | TtsA exerts its activity at the bacterial poles. a, *S.* Typhi wild type and the isogenic Δ*ttsA* mutant were grown in TTIM for 24 h, and metabolically labelled by the addition of alkyne-D-alanine (2 mM) for 240 min. Fixed bacteria were treated with an azido-AF488 fluorophore (10 μM), which was linked by click chemistry to alkyne-D-alanine that had been incorporated into the PG layer. **b**,**c**, Growth-phase dependency of the PG remodelling at the bacterial poles. *S.* Typhi wild type and isogenic Δ*ttsA* mutant were grown for 24 h in TTIM, and subsequently labelled metabolically by the addition of alkyne-D-alanine (2 mM) for 240 min. Bacteria cultures were then split into TTIM (mock) (**c**) or into TTIM containing 1% casamino acids (both conditions in the presence of alkyne-D-alanine) (**b**), which allows bacteria to re-enter the cell cycle (Supplementary Fig. 10). At the indicated time points bacteria were harvested and PG was labelled as indicated above. The scatter plots in **a**–**c** show the results of the line scan analysis of fluorescence intensity along the axes of individual bacterial cells as described in Fig. 3. Blue or red lines depict the average fluorescence from each measured point. Bar graphs show the average ratios of the signal intensities at the measuring point furthest from the centre (1.0) to the measuring point at the centre of each bacterium (0) (**$P < 0.01$; ***$P < 0.001$; ****$P < 0.0001$; NS, differences not statistically significant, $p = 0.0545$, two-sided Student's *t*-test) (Supplementary Data Set 4). **d**, TtsA localization after regrowth of *S.* Typhi (TtsA-FLAG) in casamino acid-supplemented TTIM as described above. Bacteria were fixed, treated with lysozyme (50 μg ml^{-1}) and Triton X-100 (0.3%). TtsA was visualized by fluorescence microscopy as described in Fig. 3. The scatter plot shows the line scan analysis of fluorescence intensity along the axes of individual bacterial cells as described in Fig. 3. The bar graph shows quantification of the signal intensities at the measuring point furthest from the centre (1.0), and at the centre of each bacterium (0). Numbers represent mean ± s.e.m. from 1,800 measurements (****$P < 0.0001$, two-sided Student's *t*-test) (Supplementary Data Set 4). Scale bar (**d**), 5 μm.

which is permissive for TtsA activity. We found that while the PG of wild-type *S.* Typhi grown under these conditions exhibited a significant amount of tripeptides and 3–3 (*m*-DAP–*m*-DAP) crosslinks, these crosslinks were not detect in the Δ*ycbB* mutant (Fig. 6a and Supplementary Table 1). Consistent with these observations we found that expression of a form of TtsA containing a Sec-dependent secretion signal (ssTtsA) in *S.* Typhi (for its efficient delivery into the periplasm) led to a significant reduction in c.f.u. (presumably due to deleterious effects affecting viability or growth) after growth in TTIM, which leads to a PG structure containing a significant amount of 3–3 crosslinks (Fig. 6b and Supplementary Fig. 14). In contrast, such an effect was not observed when ssTtsA was expressed in a Δ*ycbB* mutant grown under the same conditions, or in wild-type *S.* Typhi grown in LB broth (Fig. 6b and Supplementary Fig. 14), a condition that leads to a reduced amount of 3–3 crosslinks[33]. These results indicate that TtsA cannot exert its toxic effect in PG that is not rich in 3–3 crosslinks. We then tested the in vitro enzymatic activity of purified TtsA on PG obtained from wild-type or Δ*ycbB S.* Typhi strains grown under different conditions and using two different assays. We found that while TtsA was able to hydrolyse *S.* Typhi PG from wild-type bacteria grown in TTIM, no TtsA-mediated hydrolysis was detected in PG from wild-type bacteria grown in LB to logarithmic phase (conditions incompatible with TtsA activity), or in PG from the Δ*ycbB* mutant grown under any condition (Fig. 6c,d), while lysozyme was able to hydrolyse all PG preparations (Fig. 6c,d). Taken together, these results indicate that the TtsA activity is strictly exerted on YcbB-edited PG at the bacterial poles and that it most likely requires 3–3 crosslinked PG to exert its hydrolytic activity.

Discussion

Gram-negative bacteria have evolved multiple secretion mechanisms of varying complexities to transport proteins across the bacterial envelope[1–4]. While some protein secretion machines can move their substrates through all the layers of the bacterial envelope in one step, others operate by engaging the substrates in the bacterial periplasm after their translocation by the Sec machinery. We have described here a mechanism of protein translocation across the bacterial envelope responsible for the export of *S.* Typhi's typhoid toxin (Fig. 6e). Through this mechanism, the individual subunits of the toxin are first secreted to the periplasm by the Sec machinery, where they assemble into the holotoxin complex. The holotoxin is then translocated across the PG layer to a compartment on the *trans* side of the PG layer. We propose that translocation of the toxin to this compartment positions it so that it can be released in the presence of specific agonists with the capacity to infringe minor disruption to

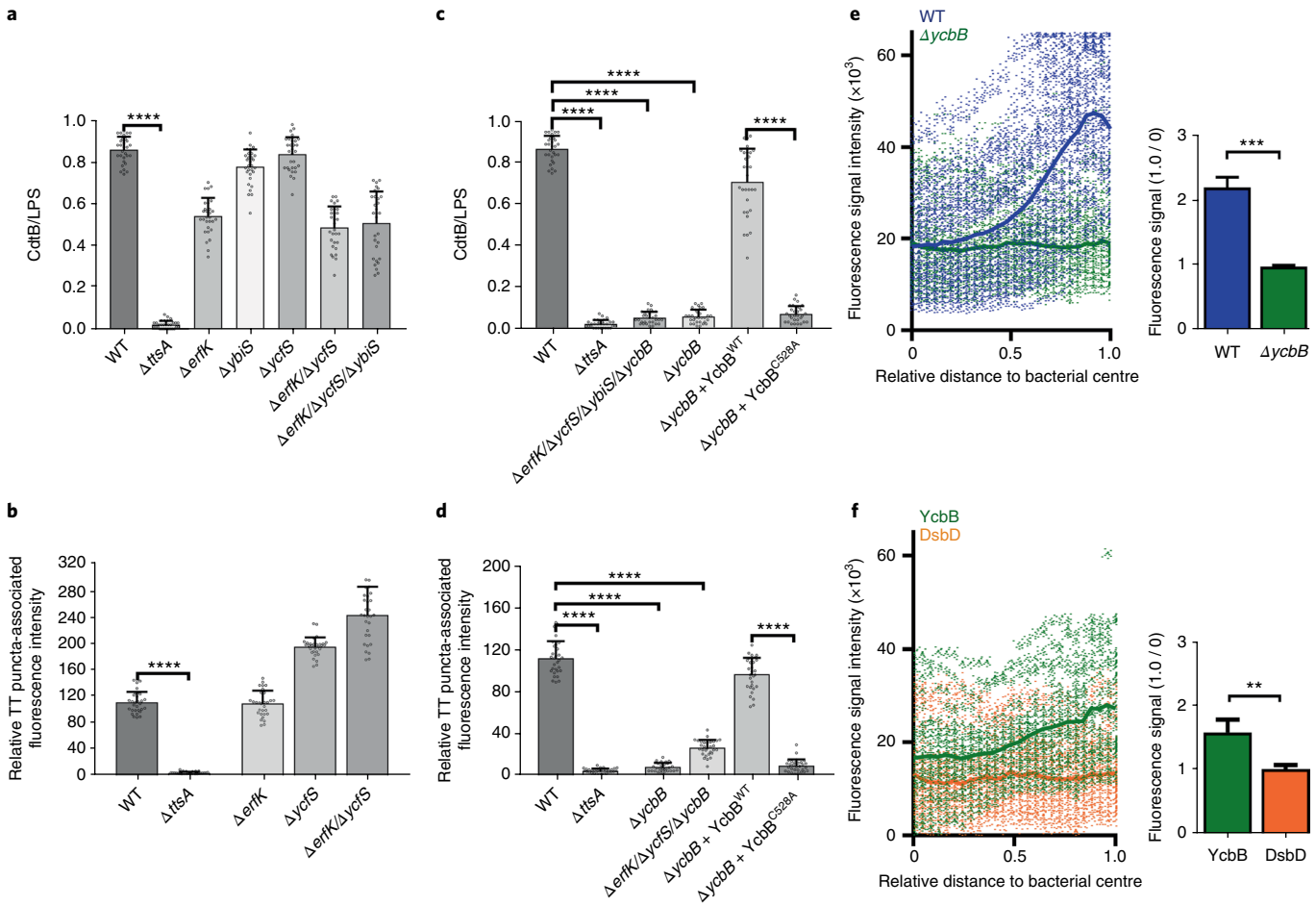

Fig. 5 | YcbB-dependent PG editing is required for typhoid toxin translocation across the bacterial envelope. a–**d**, Contribution of LD-transpeptidases to typhoid toxin translocation. *S.* Typhi (CdtB-FLAG) strains carrying the indicated mutations were grown for 24 h in TTIM, fixed, and stained as indicated in Fig. 3. The average ratios of the green/red fluorescence intensity ± s.d. are shown (****$P < 0.0001$, two-sided Student's *t*-test) (Supplementary Data Set 5) (**a**,**c**). Alternatively, Henle-407 cells were infected with the indicated *S.* Typhi strains and 24 h post infection the infected cells were fixed and stained as indicated in Fig. 3. Quantification of the fluorescence intensity of typhoid toxin (TT)-associated fluorescent puncta in infected cells is shown in **b** and **d**. Values represent relative fluorescence intensity and are presented as mean ± s.d. (****$P < 0.0001$, two-sided Student's *t*-test) (Supplementary Data Set 5). **e**, YcbB-dependent polar remodelling of the PG layer. *S.* Typhi wild-type or isogenic Δ*ycbB* mutant were grown in TTIM for 24 h, and metabolically labelled by the addition of alkyne-D-alanine (2 mM) for 240 min as indicated in Fig. 4. The scatter plot shows the results of the line scan analysis of fluorescence intensity along the axes of individual bacterial cells for wild-type (blue) and Δ*ycbB* (green) *S.* Typhi strains, carried out as described in Fig. 2. Blue or green lines depict the average of the intensities measured at each of the measuring points. The bar graph shows the average ratios of the signal intensities measured at the point furthest from the centre (1.0) to the signal intensities measured at the centre (0) of each bacterium. Numbers represent mean ± s.d. from 1,800 measurements (***$P < 0.001$, two-sided Student's *t*-test) (Supplementary Data Set 5). **f**, YcbB is enriched at the bacterial poles. *S.* Typhi (YccB-FLAG) strains expressing FLAG-tagged YcbB (green) or DsbD (orange) were grown for 24 h in TTIM, fixed, and stained with a mouse antibody directed to the FLAG-epitope. The scatter plot shows the fluorescence signal intensities and average intensities (lines) for the indicated proteins as described in Fig. 3. The bar graph shows the average ratios of the signal intensities measured at the point furthest from the centre (1.0) to the signal intensities measured at the centre (0) of each bacterium. Numbers represent mean ± s.d. from 1,800 measurements (**$P < 0.01$, two-sided Student's *t*-test) (Supplementary Data Set 5). All data in **a**–**f** were derived from at least three independent experiments.

the bacterial outer membrane. The specific nature of such agonist(s) is not known and may vary depending on the specific environments in which *S.* Typhi resides during infection. However, we have shown here that sub-inhibitory amounts of antimicrobial peptides or bile salts, which are readily encountered by *S.* Typhi during infection, are capable of efficiently triggering the release of the toxin. Therefore, it is likely that these compounds may be functionally relevant triggers of typhoid toxin release during *S.* Typhi infection. Of note, it has been reported that the release of a *Zymomonas mobilis* extracellular levansucrase, a process that depends on ZlyS[37,38], a homologue of TtsA, can be also stimulated by the presence of membrane active compounds[39].

We demonstrated that typhoid toxin translocation occurs at the bacterial poles and depends on the activity of TtsA, a specialized muramidase, which is also located at the bacterial poles. The activity of TtsA requires the specific edition of PG by the LD-transpeptidase YcbB, which catalyses the so-called 3–3 (or LD) crosslinks. Consistent with this observation, no typhoid toxin secretion or translocation to the *trans* side of the PG layer was observed in the absence of YcbB. This is remarkable in that it has been reported that, at least in *E. coli*, the vast majority (up to 98%) of the PG crosslinks are between D-Ala and *m*-DAP, the so-called 4–3 (or DD) crosslinks. However, these observations have been made with bacteria grown exponentially in rich medium, conditions that differ substantially from those encountered by intracellular bacteria (or bacteria grown in TTIM medium). In fact, there is evidence suggesting that the PG structure of intracellularly localized *Salmonella* may differ from

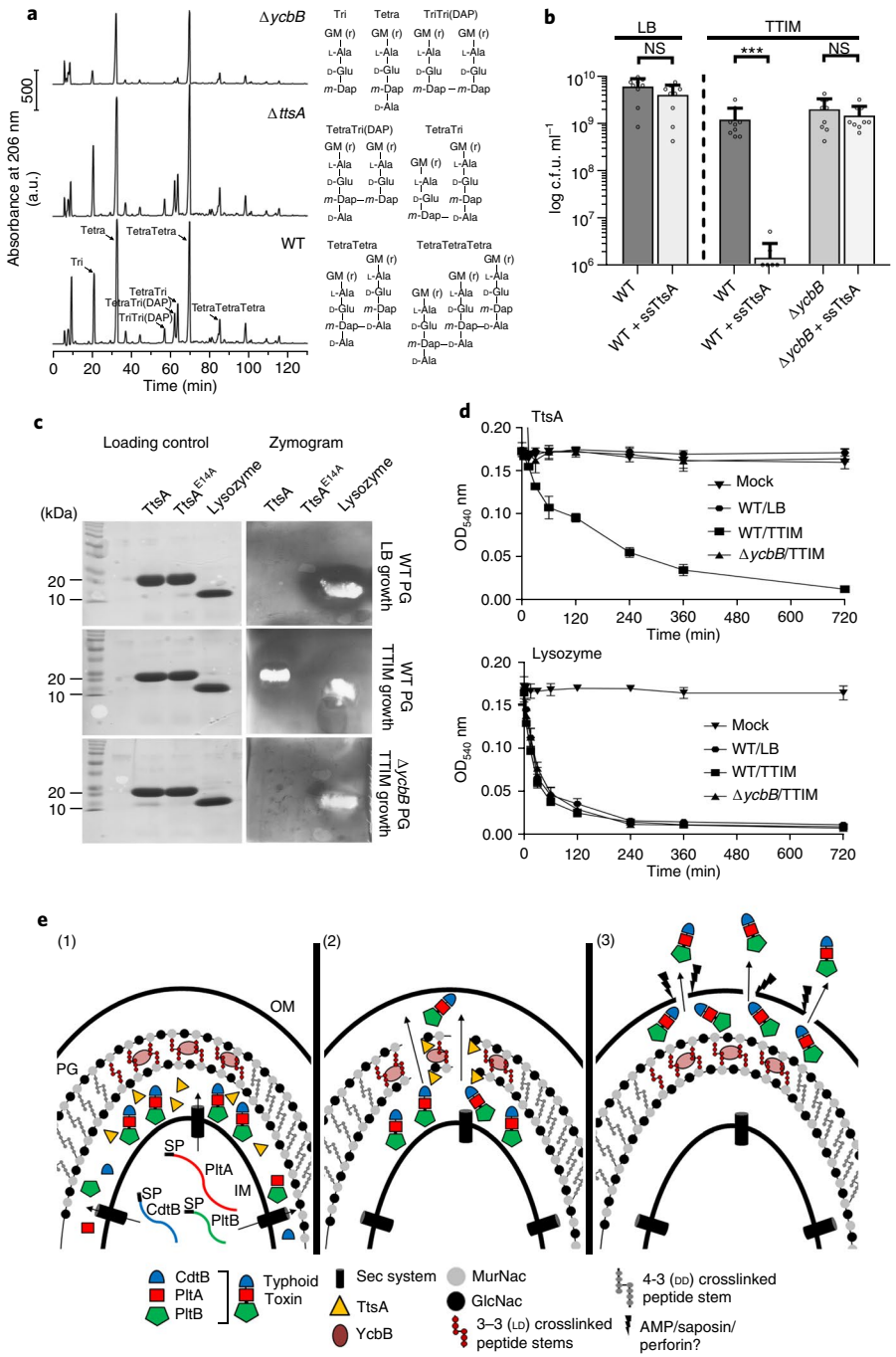

Fig. 6 | TtsA activity requires YcbB-mediated PG editing. a, Muropeptide profiles of different *S.* Typhi strains showing YcbB-dependent PG editing. The indicated *S.* Typhi strains were grown for 24 h in TTIM, and PG was isolated and analysed by high-performance liquid chromatgraphy–mass spectrometry (HPLC–MS). The *ycbB* mutant shows a significant decrease in the monomeric disaccharide tripeptide (Tri) and the 3–3 crosslinked muropeptides TriTri(DAP) and TetraTri(DAP). **b**, YcbB-dependent growth arrest after *sec*-dependent TtsA translocation to the periplasmic space. *S.* Typhi wild type and the Δ*ycbB* isogenic mutant strain, both carrying a plasmid expressing *ttsA* containing a *sec*-secretion signal (sec-TtsA) under the control of an arabinose-inducible promoter, were grown in LB or TTIM media containing 0.001% arabinose, and the number of c.f.u. was determined after 24 h of growth. Values represent mean ± s.d. (***$P < 0.001$; NS, difference not statistically significant, $P = 0.1367$ and $P = 0.316$, two-sided Student's *t*-test). **c**,**d**, TtsA muramidase activity is dependent on YcbB. PG was isolated from wild-type *S.* Typhi grown in either LB or TTIM, or from the Δ*ycbB* S. Typhi mutant grown in TTIM, as indicated. In-gel digestion zymograms were performed with equal amounts of purified wild-type TtsA, the catalytic mutant $TtsA^{E14A}$ or lysozyme (shown in a Coomassie-stained PAGE, left panels) (**c**). Alternatively, the activity of purified TtsA and lysozyme (as a control) was evaluated using a turbidimetric assay using purified PG as indicated above (**d**). Graphs show the mean turbidity (measured at OD_{540}) ± s.d. All data in **a–d** were derived from at least three independent experiments. **e**, Model for the typhoid toxin secretion mechanism. The different subunits of typhoid toxin (PltB, PltA and CdtB) are secreted to the *cis* side of the periplasm by the *sec* pathway, where they assemble into the holotoxin complex (1). The muramidase TtsA introduces a fenestration in the YcbB-modified PG layer at the bacterial poles, allowing the passage of typhoid toxin to the *trans* side of the periplasmic space, positioning the toxin in close proximity to the outer membrane (2), from where it is released to the exterior following minor disruptions to the outer membrane caused by various agonists encountered by *S.* Typhi during infection (3).

that of bacteria grown exponentially in LB broth[33,40]. Our results also suggest that the PG structure at the poles in bacteria grown under TTIM conditions may differ from the structure elsewhere in the bacterial body. The specialized location of typhoid toxin in the *trans* side of the PG at the bacterial poles also raises the intriguing possibility that in some specific environments such as the *Salmonella*-containing vacuole the bacterial envelope itself, and in particular the architecture of the periplasmic space, may be distinct. Most knowledge about bacterial physiology or the architecture of its envelope is largely derived from studies of bacteria grown in artificial rich media. However, throughout their entire life cycle bacterial pathogens inhabit environments that differ substantially from those of the media routinely used in the laboratory. Consequently, more studies are required to understand the composition and architecture of the bacterial envelope under environmental conditions that mimic those encountered by bacterial pathogens.

The protein export mechanism described here differs significantly in its evolutionary design from other two-step protein secretion systems that mediate the transport of Sec-translocated substrates[2–4]. Indeed, all two-step protein secretion systems known today engage their substrates in what would be considered the *cis* side of the PG in the periplasmic space and utilize various specific outer-membrane protein channels to move their substrates through the outer membrane. It is intriguing that all the necessary elements to build the different secretion machines are always encoded within a common gene cluster, which sometimes, although not always, also encodes the cognate secretion substrates. In contrast, other than *ttsA*, no other genes required for typhoid toxin secretion are present within the pathogenicity islet that harbours *ttsA* and the typhoid toxin genes. Furthermore, despite close scrutiny, we have been unable to identify additional *S.* Typhi genes required for typhoid toxin secretion. Periplasmic proteins can be released to the extracellular space in outer membrane vesicles (OMVs) that are shed from bacterial cells[41,42]. However, we have been unable to detect OMVs containing typhoid toxin in *S.* Typhi grown under the conditions used in these studies or in intracellularly localized *S.* Typhi. Furthermore, in infected cells, the packaging of typhoid toxin into vesicle carrier intermediates requires the interaction of PltB with a glycan receptor on the luminal side of the membrane of the *Salmonella*-containing vacuole[15]. The topology of potential toxin-containing OMVs would therefore be incompatible with this packaging mechanism. Consequently, it is unlikely that OMVs play a role in the release of typhoid toxin from *S.* Typhi cells.

Phylogenetic and genetic analyses[16] indicate that TtsA appears to be a recent exaptation of related enzymes that are utilized by bacteriophages to exit from infected bacterial cells[43]. Given the presence of homologous muramidases encoded in close proximity to bacterial toxins or large extracellular enzymes in other bacterial genomes[16,37,38,44], we predict that this protein secretion mechanism is likely to be conserved in other bacteria. We hypothesize that this recently evolved export system provides bacterial pathogens with the unique advantage of releasing pre-synthesized toxins following the reception of environmental cues (for example, antimicrobial peptides) whose presence itself may define the very specific environment in which the toxin must exert its function.

Methods

Bacterial strains and plasmids. The bacterial strains and plasmids used in this study are listed in Supplementary Table 2. All *S.* Typhi strains were derived from the clinical isolate ISP2825[45]. All in-frame deletions or insertions into the *S.* Typhi chromosome were generated by standard recombinant DNA and allelic exchange procedures using *E. coli* β-2163 *Δnic35* as the conjugative donor strain[46] and the R6K-derived suicide vector pSB890 as previously described[47]. For *S.* Typhi Δ*ttsA* complementation studies, we used plasmid pSB3783, which encodes an arabinose-inducible promoter and is derived from plasmid pBAD24[48]. For TtsA expression for protein purification we used the expression plasmid pET28b (Invitrogen) in *E. coli* strain BL21. All plasmids used in this study were constructed using the Gibson assembly cloning strategy[49]. All generated plasmids and strains used in this study have been verified by nucleotide sequencing.

Bacterial and eukaryotic cell culture. *S.* Typhi strains were routinely cultured in L broth (LB) on a rotation wheel at 37 °C. For in vitro typhoid toxin secretion assays, bacteria were subcultured in a chemically defined medium, which induces typhoid toxin expression and therefore is referred to as TTIM (typhoid toxin induction medium). This defined medium was adapted from previous studies[14,17] and its composition is as follows: K_2SO_4 (0.5 mM), KH_2PO_4 (1 mM), $(NH_4)_2SO_4$ (7.5 mM), Tris base (50 mM), Bis Tris (50 mM), casamino acids (0.1%), KCl (5 mM), cysteine (50 μg ml^{-1}), tryptophan (50 μg ml^{-1}), glycerol (32.5 mM) and magnesium (15 μM). For host cell infection assays, bacteria were subcultured in LB containing 0.3 M NaCl to stimulate expression of the SPI-1 type III secretion system[50]. When appropriate, ampicillin (100 μg ml^{-1}), kanamycin (50 μg ml^{-1}) and tetracycline (10 μg ml^{-1}) were added to the bacterial cultures. Henle-407 human intestinal epithelial cells (obtained from the Roy Curtiss III collection in 1987) were grown in Dulbecco's modified Eagle medium (DMEM, Gibco) supplemented with 10% bovine calf serum (BCS, Gemini Bioproducts) at 37 °C with 5% CO_2 in a humidified incubator. Cells were routinely tested for the presence of mycoplasma by a standard PCR method. The cells were also frequently checked for their morphological features, growth characteristics and functionalities, but were not authenticated by short tandem repeat (STR) profiling.

In vitro typhoid toxin expression and secretion assay. To detect typhoid toxin and TtsA expression in *S.* Typhi strains carrying chromosomally encoded 3×FLAG-epitope-tagged versions of CdtB (a typhoid toxin subunit) or TtsA, the different strains were grown overnight in LB, washed twice with 1× PBS (without MgCl supplement, Difco) and subcultured in TTIM after a 1:50 dilution. At the indicated time points, an equal number of bacteria (standardized by colony forming units, c.f.u.) were harvested and bacterial pellets were resuspended in Laemmli buffer and boiled for 5 min. The expression profiles of TtsA and CdtB were determined by western blot analysis using a mouse monoclonal antibody directed to the FLAG-epitope (Invitrogen). As a loading control, samples were analysed on a separate western blot with a polyclonal rabbit antibody directed to RecA.

To detect secreted typhoid toxin in bacterial supernatants, *S. Typhi* wild-type and isogenic Δ*ttsA* mutant strains, both with chromosomally encoded 3×FLAG-tagged CdtB, were grown for 24 h in TTIM to induce typhoid toxin and TtsA expression. Bacterial cultures were then mock-treated for 30 min or treated with Triton X-100 (0.1%) (Sigma-Aldrich) for 15 min, bile salts (0.05%) (Sigma-Aldrich) for 15 min, polymyxin B (0.1 μg ml^{-1}) (Sigma-Aldrich) for 10 min or C18G antimicrobial peptide (2.5 μg ml^{-1}) (AnaSpec) for 30 min. Bacterial pellets and trichloroacetic acid (TCA)-precipitated supernatants (overnight at 4 °C) were resuspended in Laemmli buffer and boiled for 5 min. The presence of typhoid toxin (CdtB subunit) in the supernatants and in the pellets was determined by western blot analyses. Cytoplasmic RecA served as a negative control for cell lyses in the supernatant analyses and as loading controls for the whole-cell lysates. Detection of secreted proteins in the bacterial supernatants by LC–MS/MS analysis after TCA precipitation (overnight at 4 °C) was carried out as described in ref. [51].

Immunofluorescence microscopy of bacteria grown in vitro. The indicated *S.* Typhi strains were grown in TTIM for 24 h and bacteria were washed with PBS and fixed using 4% paraformaldehyde (PFA) for 15 min. No fixation or other treatments were performed for the visualization of *S.* Typhi strains chromosomally encoding CdtB-sfGFP and plasmid-borne mCherry. When indicated, fixed bacteria were treated with lysozyme (Sigma-Aldrich) (50 μg ml^{-1}) for 20 min in Tris-buffer (pH 8) at 37 °C. Bacteria were then washed and mounted on glass coverslips coated with poly-D-lysine (Sigma-Aldrich). The coverslips with attached bacteria were washed with PBS and, if applicable, incubated with 1% Triton X-100 in PBS for 30 min, washed again, and incubated overnight at 4 °C with primary anti-FLAG M2 mouse monoclonal antibody (Sigma) (1:10,000) and anti-Salmonella O poly A-1 & Vi rabbit antiserum (Becton, Dickinson & Co.) (1:10,000) in PBS, containing 1% bovine serum albumin (BSA) and 0.01% Triton X-100. After removal of the primary antibody, the coverslips were washed six times with 1× PBS and incubated with secondary Alexa-Fluor 488-conjugated anti-mouse and Alexa-Fluor 594-conjugated anti-rabbit (Invitrogen) (1:2,000) antibodies in PBS, containing 1% BSA and 0.01% Triton X-100 for 60 min at room temperature (RT) protected from light. Mounted samples (ProLong Gold antifade, Molecular Probes) were visualized in an Eclipse TE2000-U (Nikon) microscope equipped with an Andor Zyla 5.5 sCMOS camera driven by Micromanager software (https://www.micro-manager.org).

***S.* Typhi cultured cell infection assays.** The different *S.* Typhi strains were grown overnight and then subcultured (1:50) in fresh LB containing 0.3 M NaCl to stimulate expression of the SPI-1 type III secretion system[50]. When bacteria reached an optical density at 600 nm (OD_{600}) of 0.9, cultured epithelial Henle-407 cells were infected for 1 h in Hank's balanced salt solution (HBSS, Gibco) at a multiplicity of infection (MOI) of 30. Cells were then washed twice with HBSS and further incubated with culture medium supplemented with gentamicin

(100 μg ml^{-1}) for 1 h to kill the remaining extracellular bacteria, and further incubated in culture medium containing gentamicin (5 μg ml^{-1}) to avoid cycles of reinfection.

Immunofluorescence microscopy of infected cultured epithelial cells. At 24 h after infection with the indicated *S.* Typhi strains, Henle-407 cells cultured on glass coverslips were rinsed with PBS and fixed with 4% paraformaldehyde for 15 min at RT. No fixation or other treatments were performed before visualization of cultured cells infected with *S.* Typhi strains expressing CdtB-sfGFP and mCherry. Samples were incubated in 50 mM NH_4Cl in PBS for 10 min and subsequently blocked in 1% BSA and 0.1% Triton X-100 in PBS for 30 min. Coverslips were washed and incubated overnight at 4 °C with primary anti-FLAG M2 mouse monoclonal antibody (Sigma) (1:10,000) and anti-*Salmonella* O poly A-1 & Vi rabbit antiserum (Becton, Dickinson & Co.) (1:10,000) in PBS, containing 1% BSA and 0.01% Triton X-100. Coverslips were then washed six times with 1× PBS and incubated for 60 min at RT (protected from light) with secondary Alexa-Fluor 488-conjugated anti-mouse and Alexa-Fluor 594-conjugated anti-rabbit (Invitrogen) (1:2,000) antibodies and 0.5 μg ml^{-1} 4′,6-diamidino-2-phenylindole (DAPI) in PBS, containing 1% BSA and 0.01% Triton X-100. Mounted samples (ProLong Gold antifade, Molecular Probes) were visualized in an Eclipse TE2000-U (Nikon) microscope equipped with an Andor Zyla 5.5 sCMOS camera driven by Micromanager software (https://www.micro-manager.org).

Quantification of fluorescence-positive bacteria after growth in vitro and within infected cells. Bacterial-associated fluorescence signals from FLAG-tagged CdtB (to visualize typhoid toxin), DsbD or SlyA were quantified by fluorescence microscopy using the open-source software ImageJ with the MicrobeJ plug-in (http://rsbweb.nih.gov/ij/)[52]. Images were captured from randomly selected fields in both the red (LPS signal to identify all bacterial cells) and green (to identify CdtB-, DsbD- or SlyA-positive bacteria) channels. The number of bacterial cells positive for green fluorescence signals (CdtB, DsbD or SlyA) was quantified relative to the total number of bacterial cells analysed (LPS signal, red). In total, 30 images were collected from which 100 randomly selected bacteria per image were analysed, resulting in 3,000 bacterial cells analysed per bacterial strain and/or condition.

Quantification of typhoid toxin-associated transport intermediates. The typhoid toxin vesicular transport intermediates were quantified by fluorescent microscopy using the open-source software ImageJ (http://rsbweb.nih.gov/ij/), as described in ref. [15]. Briefly, images were captured from randomly selected fields. Images from the LPS stain were used to identify the area corresponding to the bacterial cell body and this area was used to obtain the bacterial-associated typhoid toxin fluorescence signal, which was substracted from the typhoid toxin-associated fluorescence. The remaining fluorescence was considered to be associated with typhoid toxin carrier intermediates. Finally, the intensity of fluorescence associated with toxin carriers in each field was normalized using the fluorescence associated with typhoid toxin in bacterial cells in the same field.

Immunoelectron microscopy. An *S.* Typhi strain carrying chromosomally encoded FLAG-tagged CdtB was grown in TTMI for 24 h, fixed with 4% PFA, washed, and bacterial pellets were quickly frozen in liquid nitrogen. Alternatively, the same bacterial strain was grown in LB as indicated in section 'Immunofluorescence microscopy of infected cultured epithelial cells' to infect Henle-407 human epithelial cells, and, 24 h after infection, infected cells were fixed with 4% PFA, washed, and infected cell pellets were quickly frozen in liquid nitrogen. Samples were then processed for immunoelectron microscopy as described in ref. [53] using a mouse primary antibody (1:500), directed to the FLAG-epitopes and a secondary immunogold (8 nm)-labelled anti-mouse antibody (1:150).

Proteinase K protection assay. *S.* Typhi wild-type and Δ*ttsA* mutant strains expressing chromosomally encoded FLAG-tagged CdtB or DsbD were grown in TTIM for 24 h, washed with 1× PBS and subjected to one of two alternative procedures. In procedure 1, bacterial cells were treated with proteinase K (100 μg ml^{-1}) at 37°C for 30 min in Tris buffer (pH 8.0), washed thoroughly four times with 1× PBS to remove any remaining proteinase K, fixed with 4% PFA for 15 min at RT, and treated with lysozyme (50 μg ml^{-1}) for 20 min at 37 °C in Tris buffer (pH 8.0). In procedure 2, bacterial cells were fixed with 4% PFA for 15 min at RT, washed twice with 1× PBS, followed by mock treatment or treatment with lysozyme (50 μg ml^{-1}) for 20 min at 37 °C in Tris buffer (pH 8.0), washed twice with 1× PBS, followed by mock treatment or treatment with proteinase K (100 μg ml^{-1}) for 30 min at 37 °C in Tris buffer pH 8.0. All samples were subsequently treated with 0.3% Triton X-100 for 30 min at RT and mounted on D-polylysine-coated coverslips. Fluorescence microscopy and quantifications of tagged-protein-associated fluorescence signals (green) normalized to the LPS signals (red) were performed as described in sections 'Immunofluorescence microscopy of bacteria grown in vitro' and 'Quantification of fluorescence-positive bacteria after growth in vitro and within infected cells'.

Fluorescence labelling of PG. *S.* Typhi wild-type, Δ*ttsA* and Δ*ycbB* mutant strains were grown in TTIM for 24 h, then incubated in TTIM containing alkyne-D-alanine (2 mM) (Boao Pharma) for 4 h. To analyse PG remodelling in bacteria that had been allowed to re-enter the cell cycle after growth to stationary phase, *S.* Typhi strains were grown to stationary phase in TTIM and labelled with alkyne-D-alanine as described above. Bacterial cultures were then split, casamino acids or eluent were added, and cultures were further grown for the indicated times (always in the presence of alkyne-D-alanine). In all cases, after the various growth conditions bacteria were washed with PBS and fixed for 15 min in 4% PFA at RT. Fixed bacteria were resuspended in Click-iT Cell Reaction Buffer (Invitrogen), and copper-catalysed click chemistry was performed in the dark at RT for 30 min using the Click-iT Cell Reaction Kit (Invitrogen) with 10 μM azido-Alexa-Fluoro 488 fluorophore (Invitrogen). Bacteria were then washed three times and attached to poly-D-lysine-coated coverslips. If applicable, bacterial cells were counterstained for LPS (red) with primary anti-*Salmonella* O poly A-1 & Vi rabbit antiserum (Becton, Dickinson & Co.) (1:10,000) and secondary anti-rabbit Alexa-Fluor594 (Invitrogen) (1:2,000) antibody.

Fluorescence distribution analyses. Line scan analysis of the distribution of fluorescence signal intensities of labelled PG or stained bacteria along the medial axes of the bacterial cell bodies was carried out using the MicrobeJ plug-in[52] of ImageJ (https://imagej.nih.gov/ij/index.html) software. Random fluorescence microscopy images were obtained and bacterial cells were defined as regions of interest (ROI) by using LPS (red) counterstaining. The centre within each ROI was identified and 26 measuring points along the medial axes of the bacteria from the centre (0) to each of the poles (1.0) were automatically selected on the PG or labelled antibody fluorescence channels (green). For the PG-associated fluorescence distribution analysis, the fluorescence signal associated with non-TtsA-dependent PG labelling was substracted.

TtsA protein purification. The coding sequence for *ttsA* was amplified from *S.* Typhi strain ISP2825 and cloned by the Gibson cloning strategy[49] into the expression vector pET28a+ (Novagen), resulting in N-terminal his-epitope tagged TtsA. Expression and purification of TtsA^{WT} and catalytic mutant TtsA^{E14A} were carried out as described in ref. [11]. *E. coli* strain BL21 carrying the different plasmids were grown in LB containing kanamycin (50 μg ml^{-1}) to an OD_{600} of 0.6–0.7 at 37 °C. Expression of TtsA was subsequently induced by the addition of 0.5 mM isopropyl β-D-1-thiogalactopyranoside (IPTG), and induced cultures were incubated overnight at 25 °C. Bacterial cells were pelleted by centrifugation, resuspended in lysis buffer (Tris–HCl (150 mM, pH 8.0), NaCl (100 mM), imidazol (10 mM), lysozyme (100 μg ml^{-1}), DNAse (100 μg ml^{-1}), saturated phenylmethylsulfonyl fluoride (PMSF) and lysed with a French press. Lysates were subsequently pelleted (20,000*g* 1 h, 4 °C), and affinity-purified using a nickel resin (Qiagen) column. The eluates were diluted in 20 mM Tris–HCl, pH 8.0 buffer and loaded onto a Hi Trap Q ion-exchange column. Fractions from the ion-exchange chromatography were monitored on SDS–PAGE, concentrated, and further purified using a Superdex 200 column. Final fractions were examined for purity on a 12% SDS–PAGE.

PG hydrolysis assays. *S.* Typhi wild-type and Δ*ycbB* mutant strains were grown in TTIM for 24 h or, when indicated, in LB to logarithmic growth phase (OD_{600} 0.5), and PG was then isolated as previously described[54]. Purified PG preparations were resuspended in MilliQ water containing 0.01% NaN_3 and stored at 4 °C until their use in different assays. Muramidase activity of purified TtsA was detected by in-gel digestion (zymographic assay) or by a turbidimetry assay. For the zymogram assay, purified TtsA (10 μg), its catalytic mutant TtsA^{E14A} (10 μg) or lysozyme (10 μg) were separated on 12% low SDS (0.01%) polyacrylamide gels containing 0.1% (wt/vol) purified *S.* Typhi PG. Protein samples were not boiled and the sample loading buffer contained 0.1% Coomassie Blue G-250 with 150 mM 6-aminocaproic acid (ACA) but no SDS. Following electrophoresis, the gels were split in half. One half was used as protein loading control and was stained with Coomassie (0.5%). The other half was used for the zymogram assay. In this case the gels were rinsed and soaked in water twice for 5 min at room temperature, incubated twice for 1 h in washing buffer (100 mM Tris–HCl (pH 8.0), 1% (vol/vol) Triton X-100) at RT with gentle agitation, rinsed and soaked twice with water for 5 min, and subsequently incubated overnight at 37 °C in enzyme activity buffer (20 mM Tris–HCl (pH 6.8) and 50 mM NaCl) with gentle agitation. Gels were stained for PG with 0.1% (wt/vol) methylene blue in 0.01% (wt/vol) KOH, and, after de-staining with water, the unstained bands due to local degradation of PG appeared as a clear zone in a blue background of stained PG. The turbidimetric assay was performed with the same highly purified PG preparation as used for the zymographic assay. Isolated PG was diluted in enzyme activity buffer (20 mM Tris–HCl (pH 6.8), 50 mM NaCl) to an OD_{540} of ~0.175. Purified TtsA, TtsA^{E14A} or lysozyme (5 μg of each) were added to the buffer and optical densities measurements at 540 nm were performed at the indicated time points.

Bacterial growth arrest assay. *S.* Typhi wild-type and Δ*ycbB* mutant strains, expressing plasmid-born TtsA containing an N-terminal Sec translocation signal sequence from DsbA under the control of an arabinose-inducible promoter, were grown overnight in LB medium supplemented with 5 μg ml^{-1} tetracycline. Overnight grown bacteria were subcultured (1:50) in TTIM or LB and grown to an

OD_{600} of 0.3, at which point 0.001% arabinose was added to the bacterial cultures to induce the expression of TtsA, and further incubated for 20 h. Colony forming units were then determined by plating bacterial dilutions on LB agar plates.

HPLC–MS analyses of isolated *S.* Typhi PG. PG was isolated and analysed according to a previously described procedure[55].

Reporting summary. Further information on research design is available in the Nature Research Reporting Summary linked to this article.

Data availability

All data generated or analysed during this study are included in this published article and its Supplementary Information.

Received: 23 April 2018; Accepted: 20 August 2018;
Published online: 24 September 2018

References

1. Galán, J. & Waksman, G. Protein-injection machines in bacteria. *Cell* **172**, 1306–1318 (2018).
2. Costa, T. et al. Secretion systems in Gram-negative bacteria: structural and mechanistic insights. *Nat. Rev. Microbiol.* **13**, 343–359 (2015).
3. Green, E. & Mecsas, J. in *Virulence Mechanisms of Bacterial Pathogens* 5th edn (eds Kudva, I. et al.) 215–239 (ASM Press, Washington, DC, 2016).
4. Koster, M., Bitter, W. & Tommassen, J. Protein secretion mechanisms in Gram-negative bacteria. *Int. J. Med. Microbiol.* **290**, 325–331 (2000).
5. Parry, C., Hien, T. T., Dougan, G., White, N. & Farrar, J. Typhoid fever. *N. Engl. J. Med.* **347**, 1770–1782 (2002).
6. Crump, J. & Mintz, E. Global trends in typhoid and paratyphoid fever. *Clin. Infect. Dis.* **50**, 241–246 (2010).
7. Raffatellu, M., Wilson, R., Winter, S. & Bäumler, A. Clinical pathogenesis of typhoid fever. *J. Infect. Dev. Ctries* **2**, 260–266 (2008).
8. Wain, J., Hendriksen, R., Mikoleit, M., Keddy, K. & Ochiai, R. Typhoid fever. *Lancet* **385**, 1136–1145 (2015).
9. Dougan, G. & Baker, S. *Salmonella enterica* serovar Typhi and the pathogenesis of typhoid fever. *Annu. Rev. Microbiol.* **68**, 317–336 (2014).
10. Spano, S., Ugalde, J. E. & Galan, J. E. Delivery of a *Salmonella* Typhi exotoxin from a host intracellular compartment. *Cell Host Microbe* **3**, 30–38 (2008).
11. Song, J., Gao, X. & Galan, J. E. Structure and function of the *Salmonella* Typhi chimaeric A_2B_5 typhoid toxin. *Nature* **499**, 350–354 (2013).
12. Galan, J. E. Typhoid toxin provides a window into typhoid fever and the biology of *Salmonella* Typhi. *Proc. Natl Acad. Sci. USA* **113**, 6338–6344 (2016).
13. Haghjoo, E. & Galan, J. E. *Salmonella* Typhi encodes a functional cytolethal distending toxin that is delivered into host cells by a bacterial-internalization pathway. *Proc. Natl Acad. Sci. USA* **101**, 4614–4619 (2004).
14. Fowler, C. & Galán, J. Decoding a *Salmonella* Typhi regulatory network that controls typhoid toxin expression within human cells. *Cell Host Microbe* **23**, 65–76 (2018).
15. Chang, S., Song, J. & Galán, J. Receptor-mediated sorting of typhoid toxin during its export from *Salmonella* Typhi-infected cells. *Cell Host Microbe* **20**, 682–689 (2016).
16. Hodak, H. & Galán, J. *Salmonella* Typhi homolog of bacteriophage muramidases controls typhoid toxin secretion. *EMBO Rep.* **14**, 95–102 (2013).
17. Beuzón, C., Banks, G., Deiwick, J., Hensel, M. & Holden, D. pH-dependent secretion of SseB, a product of the SPI-2 type III secretion system of *Salmonella typhimurium*. *Mol. Microbiol.* **33**, 806–816 (1999).
18. Spanò, S. & Galán, J. A Rab32-dependent pathway contributes to *Salmonella* Typhi host restriction. *Science* **338**, 960–963 (2012).
19. Darmoise, A., Maschmeyer, P. & Winau, F. The immunological functions of saposins. *Adv. Immunol.* **105**, 25–62 (2010).
20. McCormack, R. et al. Perforin-2 is essential for intracellular defense of parenchymal cells and phagocytes against pathogenic bacteria. *eLife* **4**, e06508 (2015).
21. Prost, L., Sanowar, S. & Miller, S. Salmonella sensing of anti-microbial mechanisms to promote survival within macrophages. *Immunol. Rev.* **219**, 55–65 (2007).
22. Di Domenico, E., Cavallo, I., Pontone, M., Toma, L. & Ensoli, F. Biofilm producing *Salmonella* Typhi: chronic colonization and development of gallbladder cancer. *Int. J. Mol. Sci.* **18**, E1887 (2017).
23. Gunn, J. et al. *Salmonella* chronic carriage: epidemiology, diagnosis, and gallbladder persistence. *Trends Microbiol.* **22**, 648–655 (2014).
24. Porat, A., Cho, S. & Beckwith, J. The unusual transmembrane electron transporter DsbD and its homologues: a bacterial family of disulfide reductases. *Res. Microbiol.* **155**, 617–622 (2004).
25. Siegrist, M. et al. D-Amino acid chemical reporters reveal peptidoglycan dynamics of an intracellular pathogen. *ACS Chem. Biol.* **8**, 500–505 (2013).
26. Turner, R., Vollmer, W. & Foster, S. Different walls for rods and balls: the diversity of peptidoglycan. *Mol. Microbiol.* **91**, 862–874 (2014).
27. Egan, A., Biboy, J., van't Veer, I., Breukink, E. & Vollmer, W. Activities and regulation of peptidoglycan synthases. *Philos. Trans. R. Soc. Lond. B* **370**, 20150031 (2015).
28. Vollmer, W., Blanot, D. & de Pedro, M. A. Peptidoglycan structure and architecture. *FEMS Microbiol. Rev.* **32**, 149–167 (2008).
29. Cameron, T., Anderson-Furgeson, J., Zupan, J., Zik, J. J. & Zambryski, P. Peptidoglycan synthesis machinery in *Agrobacterium tumefaciens* during unipolar growth and cell division. *mBio* **5**, 14 (2014).
30. Kuru, E., Tekkam, S., Hall, E., Brun, Y. & Van Nieuwenhze, M. Synthesis of fluorescent D-amino acids and their use for probing peptidoglycan synthesis and bacterial growth in situ. *Nat. Protoc.* **10**, 33–52 (2015).
31. Glauner, B., Holtje, J. V. & Schwarz, U. The composition of the murein of *Escherichia coli*. *J. Biol. Chem.* **263**, 10088–10095 (1988).
32. Holtje, J. V. Growth of the stress-bearing and shape-maintaining murein sacculus of *Escherichia coli*. *Microbiol. Mol. Biol. Rev.* **62**, 181–203 (1998).
33. Quintela, J., de Pedro, M., Zöllner, P., Allmaier, G. & Garcia-del Portillo, F. Peptidoglycan structure of *Salmonella typhimurium* growing within cultured mammalian cells. *Mol. Microbiol.* **23**, 693–704 (1997).
34. Magnet, S. et al. Identification of the L,D-transpeptidases responsible for attachment of the Braun lipoprotein to *Escherichia coli* peptidoglycan. *J. Bacteriol.* **189**, 3927–3931 (2007).
35. Magnet, S., Dubost, L., Marie, A., Arthur, M. & Gutmann, L. Identification of the L,D-transpeptidases for peptidoglycan cross-linking in *Escherichia coli*. *J. Bacteriol.* **190**, 4782–4785 (2008).
36. Alcorlo, M., Martinez-Caballero, S., Molina, R. & Hermoso, J. A. Carbohydrate recognition and lysis by bacterial peptidoglycan hydrolases. *Curr. Opin. Struct. Biol.* **44**, 87–100 (2017).
37. Kondo, Y. et al. Cloning and characterization of a pair of genes that stimulate the production and secretion of *Zymomonas mobilis* extracellular levansucrase and invertase. *Biosci. Biotechnol. Biochem.* **58**, 526–530 (1994).
38. Oda, Y., Yanase, H., Kato, N. & Tonomura, K. Liberation of sucrose-hydrolyzing enzymes from cells by the zliS gene product that mediates protein secretion in *Zymomonas mobilis*. *J. Ferment. Bioeng.* **77**, 419–422 (1994).
39. Takeda, K. et al. The effect of amphiphilic compounds on the secretion of levansucrase by *Zymomonas mobilis*. *Process Biochem.* **40**, 3723–3731 (2005).
40. Rico-Pérez, G. et al. A novel peptidoglycan D,L-endopeptidase induced by *Salmonella* inside eukaryotic cells contributes to virulence. *Mol. Microbiol.* **99**, 546–556 (2016).
41. Takeda, K., Guerrero-Mandujano, A., Hernández-Cortez, C., Ibarra, J. & Castro-Escarpulli, G. The outer membrane vesicles: secretion system type zero. *Traffic* **18**, 425–432 (2017).
42. Schwechheimer, C. & Kuehn, M. Outer-membrane vesicles from Gram-negative bacteria: biogenesis and functions. *Nat. Rev. Microbiol.* **13**, 605–619 (2015).
43. Wang, I., Smith, D. & Young, R. Holins: the protein clocks of bacteriophage infections. *Annu. Rev. Microbiol.* **54**, 799–825 (2000).
44. Hamilton, J. et al. A holin and an endopeptidase are essential for chitinolytic protein secretion in *Serratia marcescens*. *J. Cell Biol.* **207**, 615–626 (2014).
45. Galan, J. E. & Curtiss, R. III Distribution of the *invA, -B, -C,* and *-D* genes of *Salmonella typhimurium* among other *Salmonella* serovars: *invA* mutants of *Salmonella Typhi* are deficient for entry into mammalian cells. *Infect. Immun.* **59**, 2901–2908 (1991).
46. Demarre, G. et al. A new family of mobilizable suicide plasmids based on broad host range R388 plasmid (IncW) and RP4 plasmid (IncPα) conjugative machineries and their cognate *Escherichia coli* host strains. *Res. Microbiol.* **156**, 245–255 (2005).
47. Kaniga, K., Bossio, J. C. & Galan, J. E. The *Salmonella typhimurium* invasion genes *invF* and *invG* encode homologues of the AraC and PulD family of proteins. *Mol. Microbiol.* **13**, 555–568 (1994).
48. Guzman, L. M., Belin, D., Carson, M. J. & Beckwith, J. Tight regulation, modulation, and high-level expression by vectors containing the arabinose PBAD promoter. *J. Bacteriol.* **177**, 4121–4130 (1995).
49. Gibson, D. G. et al. Enzymatic assembly of DNA molecules up to several hundred kilobases. *Nat. Methods* **6**, 343–345 (2009).
50. Galán, J. E. & Curtiss, R. III Expression of *Salmonella typhimurium* genes required for invasion is regulated by changes in DNA supercoiling. *Infect. Immun.* **58**, 1879–1885 (1990).
51. Liu, X., Gao, B., Novik, V. & Galan, J. E. Quantitative proteomics of intracellular *Campylobacter jejuni* reveals metabolic reprogramming. *PLoS Pathog.* **8**, e1002562 (2012).
52. Ducret, A., Quardokus, E. M. & Brun, Y. V. MicrobeJ, a tool for high throughput bacterial cell detection and quantitative analysis. *Nat. Microbiol.* **1**, 16077 (2016).
53. Seemann, J., Pypaert, M., Taguchi, T., Malsam, J. & Warren, G. Partitioning of the matrix fraction of the Golgi apparatus during mitosis in animal cells. *Science* **295**, 848–851 (2002).

54. Heidrich, C. et al. Involvement of *N*-acetylmuramyl-L-alanine amidases in cell separation and antibiotic-induced autolysis of *Escherichia coli*. *Mol. Microbiol.* **41**, 167–178 (2001).
55. Glauner, B. Separation and quantification of muropeptides with high-performance liquid chromatography. *Anal. Biochem.* **172**, 451–464 (1988).

Acknowledgements

The authors thank H. Rego for useful discussions, and members of the Galán laboratory for critical review of the manuscript. T.G. was supported in part by a Postdoctoral Fellowship (GE 2653/1-1) from the Deutsche Forschungsgemeinschaft (German Research Foundation). This work was supported by the National Institute of Allergy and Infectious Diseases under grant AI079022 (to J.E.G.) and the UK Medical Research Council under grant MR/N002679/1 (to W.V.).

Author contributions

T.G. was involved in the design and interpretation of experiments and conducted all experiments shown except the biochemical characterization of the PG structure, which was conducted by M.P. with the supervision of W.V., and the LC–MS/MS analysis of culture supernatants, which was carried out by M.L.-T. J.E.G was involved in the design, interpretation and supervision of this study. T.G. and J.E.G. wrote the paper with comments from all authors.

Competing interests

The authors declare no competing interests.

Additional information

Supplementary information is available for this paper at https://doi.org/10.1038/s41564-018-0248-x.

Reprints and permissions information is available at www.nature.com/reprints.

Correspondence and requests for materials should be addressed to J.E.G.

Publisher's note: Springer Nature remains neutral with regard to jurisdictional claims in published maps and institutional affiliations.

nature research

Corresponding author(s): Jorge E. Galán

Reporting Summary

Nature Research wishes to improve the reproducibility of the work that we publish. This form provides structure for consistency and transparency in reporting. For further information on Nature Research policies, see Authors & Referees and the Editorial Policy Checklist.

Statistical parameters

When statistical analyses are reported, confirm that the following items are present in the relevant location (e.g. figure legend, table legend, main text, or Methods section).

n/a	Confirmed	
☐	☒	The exact sample size (*n*) for each experimental group/condition, given as a discrete number and unit of measurement
☐	☒	An indication of whether measurements were taken from distinct samples or whether the same sample was measured repeatedly
☐	☒	The statistical test(s) used AND whether they are one- or two-sided *Only common tests should be described solely by name; describe more complex techniques in the Methods section.*
☒	☐	A description of all covariates tested
☒	☐	A description of any assumptions or corrections, such as tests of normality and adjustment for multiple comparisons
☐	☒	A full description of the statistics including central tendency (e.g. means) or other basic estimates (e.g. regression coefficient) AND variation (e.g. standard deviation) or associated estimates of uncertainty (e.g. confidence intervals)
☒	☐	For null hypothesis testing, the test statistic (e.g. *F*, *t*, *r*) with confidence intervals, effect sizes, degrees of freedom and *P* value noted *Give P values as exact values whenever suitable.*
☒	☐	For Bayesian analysis, information on the choice of priors and Markov chain Monte Carlo settings
☒	☐	For hierarchical and complex designs, identification of the appropriate level for tests and full reporting of outcomes
☒	☐	Estimates of effect sizes (e.g. Cohen's *d*, Pearson's *r*), indicating how they were calculated
☐	☒	Clearly defined error bars *State explicitly what error bars represent (e.g. SD, SE, CI)*

Our web collection on statistics for biologists may be useful.

Software and code

Policy information about availability of computer code

Data collection	Micro-Manager open source Microscopy Software, version 1.4
Data analysis	ImageJ open source software, version 1.50i with MicrobeJ plug-in, version 5.12a[6] GraphPad Prism 7

For manuscripts utilizing custom algorithms or software that are central to the research but not yet described in published literature, software must be made available to editors/reviewers upon request. We strongly encourage code deposition in a community repository (e.g. GitHub). See the Nature Research guidelines for submitting code & software for further information.

Data

Policy information about availability of data

All manuscripts must include a data availability statement. This statement should provide the following information, where applicable:

- Accession codes, unique identifiers, or web links for publicly available datasets
- A list of figures that have associated raw data
- A description of any restrictions on data availability

The authors declare that the data supporting the findings of this study are available within the paper and its supplementary information files.

The following figures have associated raw data: figure 1, figure 2, figure 3, figure 4 and figure 5.

Field-specific reporting

Please select the best fit for your research. If you are not sure, read the appropriate sections before making your selection.

☒ Life sciences ☐ Behavioural & social sciences ☐ Ecological, evolutionary & environmental sciences

For a reference copy of the document with all sections, see nature.com/authors/policies/ReportingSummary-flat.pdf

Life sciences study design

All studies must disclose on these points even when the disclosure is negative.

Sample size	Sample sizes were empirically determined to optimize numbers based on our previous experience with equivalent experiments
Data exclusions	No data were excluded from the analyses
Replication	All attempts at replicating the results were successful
Randomization	Data were obtained by analyzing randomly selected bacteria based only on bacteria specific fluorescence signal detections
Blinding	Investigators were not blinded to group allocation during the experiments or to the outcome assessment

Reporting for specific materials, systems and methods

Materials & experimental systems

n/a	Involved in the study
☒	☐ Unique biological materials
☐	☒ Antibodies
☐	☒ Eukaryotic cell lines
☒	☐ Palaeontology
☒	☐ Animals and other organisms
☒	☐ Human research participants

Methods

n/a	Involved in the study
☒	☐ ChIP-seq
☒	☐ Flow cytometry
☒	☐ MRI-based neuroimaging

Antibodies

Antibodies used

Monoclonal ANTI-FLAG® M2 mouse antibody (Sigma-Aldrich, F1804)
Anti-Salmonella Typhi O poly A-1 & Vi rabbit antiserum (Sifin, TS1605)
Monoclonal ANTI-GFP mouse antibody (ThermoFisher Scientific, A-11121)
Anti typhoid toxin, CdtB subunit, rabbit antiserum (Pocon rabbit farm & laboratory)
Anti typhoid toxin, PltB subunit, rabbit antiserum (Pocon rabbit farm & laboratory)
Anti RecA rabbit antiserum

Validation

Monoclonal ANTI-FLAG® M2 antibody validated by the manufacturer (specification sheet statement: "detects a single band of protein on a Western Blot from mammalian crude cell lysates by chemiluminescent probing". ANTI-FLAG antibody is referenced in 400 peer-reviewed papers, accessible on the manufacture`s homepage.

Anti-Salmonella O poly A-1 & Vi rabbit antiserum validated by the manufacturer, Sifin.

Monoclonal ANTI-GFP mouse antibody validated by the manufacturer and referenced in 29 peer-review papers as stated on the manufacturer`s homepage.

Anti-typhoid toxin (CdtB and PltB subunit) rabbit antiserum (Pocon rabbit farm & laboratory) validated by Western Blot analyses with purified typhoid toxin and typhoid toxin from bacterial crude cell lysates. Validations were performed in the Galán lab.

Anti-RecA rabbit antiserum was validated and referenced in Chang, S., Song, J., and Galán, J. (2016). Receptor-Mediated Sorting of Typhoid Toxin during Its Export from Salmonella Typhi-Infected Cells. Cell Host Microbe 20, 682-689

Eukaryotic cell lines

Policy information about cell lines

Cell line source(s)	Henle-407 cells were obtained from the Roy Curtiss laboratory collection
Authentication	The cells were frequently checked for their morphological features, growth speed and functionalities, but were not authenticated by short tandem repeat (STR) profiling
Mycoplasma contamination	All cell lines tested negative for mycoplasma contamination
Commonly misidentified lines (See ICLAC register)	No commonly misidentified cell lines were used